Eur. Phys. J. B **26**, 329–338 (2002)
DOI: 10.1140/epjb/e20020097

THE EUROPEAN PHYSICAL JOURNAL B
EDP Sciences

Aging, rejuvenation, and memory phenomena in a lead-based relaxor ferroelectric

O. Kircher[1,a] and R. Böhmer[1,2,b]

[1] Institut für Physikalische Chemie, Johannes Gutenberg-Universität, 55099 Mainz, Germany
[2] Experimentelle Physik III, Universität Dortmund, 44221 Dortmund, Germany

Received 18 December 2001 and Received in final form 28 January 2002

Abstract. Isothermal aging and temperature cycle experiments were done on the relaxor ferroelectric lead magnesium niobate mixed with 10% lead titanate (PMN-10PT) around and below the diffuse maximum of the dielectric loss. With increasing aging time t_w the isothermal evolution of the *linear* susceptibility follows a power law and does not show frequency scaling. The *non-linear* susceptibility, however, obeys nearly perfect ωt_w-scaling. After aging the sample at a single temperature we observed both rejuvenation and memory effects in temperature cycle experiments. This observation indicates symmetric behavior in the sense that it shows up irrespective of whether cooling with subsequent re-heating or heating with subsequent re-cooling was performed. The memory effect is absent if subsequent to aging the temperature is increased significantly above that corresponding to the maximum in the dielectric loss. The symmetric behavior within negative and positive temperature cycles under these conditions can be rationalized by the notion of movable domain walls. These become fixed in their configuration on a large spatial scale while more flexible wall segments still show re-conformation processes when cooling or heating the sample after aging.

PACS. 77.22.-d Dielectric properties of solids and liquids – 77.84.Dy Niobates, titanates, tantalates, PZT ceramics, etc. – 61.43.-j Disordered solids

1 Introduction

Relaxor ferroelectrics (relaxors) belong to the class of materials which show strong chemical disorder. This leads to a low-temperature state with frozen-in polarization devoid of long-range ferroelectric order. Among them PMN is the prototypic substance which was first discovered by Smolensky and Agronovskaja [1]. Because of their possible technical applications, *e.g.* as multilayer ceramic capacitors [2] or as electromechanical actuators [3], there has been much interest in relaxors through recent years. From the point of view of fundamental research relaxors are challenging as examples of disordered systems.

Despite numerous experimental investigations – including linear and non-linear dielectric spectroscopy [4–9], transmission electron microscopy [10–12], light scattering [13–15], and X-ray or neutron scattering [16–19] – the microscopic origin of the unusual physical properties of relaxors still remains a point of discussion. In contrast to pure ferroelectrics they show a broad peak in the dielectric permittivity when plotted *versus* temperature. This phenomenon is often referred to as "diffuse" phase transition. Furthermore, a strong frequency dispersion of the dielectric permittivity, ε', and of the dielectric loss, ε'', in the temperature regime around the peak as well as the absence of a Curie-Weiss behavior in ε' above the peak have been observed [5,20,21].

In the past several models have been proposed to explain the dynamic properties of PMN-like and other relaxors [5,6,8,22–26]. None of those models is able to explain *all* the observed features. Therefore the question remains open whether relaxors are properly viewed (i) as disordered ferroelectric or (ii) as glassy materials similar to electric dipole glasses [27] or magnetic spin glasses [28]. In scenario (i) the dipolar dynamics is governed by movable domain walls the mobility of which is strongly reduced by pinning effects stemming from the chemical disorder present in relaxors [29]. In scenario (ii) a glasslike freezing of randomly interacting polar nanoregions occurs. To our knowledge none of the experimental results reported on relaxors so far can provide a generally-agreed-upon answer to this question.

Recently we studied the polydispersive dielectric response of the relaxor PMN-10PT with nonresonant hole burning spectroscopy, a non-linear dielectric method [30,31]. Within a temperature range around the peak of the dielectric permittivity our experimental findings could be well understood based on the notion of a disordered ferroelectric. The hole burning experiment can be

[a] *Present address*: Institut für Nanotechnologie, Forschungszentrum Karlsruhe, 76021 Karlsruhe, Germany
[b] e-mail: roland.bohmer@uni-dortmund.de

interpreted as a local variant of physical aging after generating non-equilibrium conditions by a spectrally selective energy input into the system under investigation [31–33]. We should mention that nonresonant dielectric hole burning was also applied to other highly polar dielectrics as well as to a spin glass [34–36].

In a typical aging experiment, well known from studies of disordered materials like spin glasses [28] or polymeric glass formers [37], one monitors the response of a sample that has been aged for a time t_w subsequent to causing non-equilibrium conditions. Usually one records the time-dependent isothermal evolution of the complex linear susceptibility χ after a temperature jump or after cooling the sample with a constant cooling rate to the aging temperature $T_{\rm age}$. In PLZT ceramics aging phenomena were also monitored *via* the non-linear dielectric susceptibility [38].

Generally, aging can be observed in disordered substances in temperature regimes for which the free-energy minimum is widely separated from the starting point in phase space. Due to the existence of significant barriers in the energy landscape it is impossible for the system to visit the whole phase space very quickly. As a consequence the system moves towards its thermodynamic equilibrium only slowly. These slow relaxation processes are denoted as *physical* aging [37] while *chemical* aging refers to aging processes in which the breaking of chemical bonds is involved. In this paper we exclusively study physical aging processes.

A recent investigation of the aging behavior of the dielectric susceptibility of different lead-based relaxors showed that different aging mechanisms are active in these relaxors [39]. While deep in the relaxor phase a PLZT ceramic and a single crystal of PMN revealed an aging behavior similar to that observed in spin glasses, at higher temperatures the PLZT ceramic and a PMN-30PT single crystal showed qualitatively different behavior. The aging of the susceptibility in PMN-30PT proceeded similar to the aging in disordered ferromagnets [40] which do not show memory effects on temperature cycling.

In this paper we describe the aging of the linear and likewise of the non-linear complex susceptibility in the mixed relaxor $(PbMg_{1/3}Nb_{2/3}O_3)_{1-x}(PbTiO_3)_x$ with $x = 0.1$ (PMN-10PT). Furthermore we report on our measurements dealing with the (i) isothermal aging after cooling the system with different cooling rates to the aging temperature $T_{\rm age}$, (ii) the effect of rejuvenation and memory after aging at a single temperature, and (iii) the subsequent aging at two temperatures.

2 Experimental methods

For the present study we used crystalline ceramics of PMN with a nominal admixture of 10% $PbTiO_3$ (PT) provided by the Material Research Laboratory of the Pennsylvania State University. The PMN-10PT material was found to be much less susceptible to chemical aging than pure PMN, but nevertheless retains typical relaxor properties [5,41]. It has been observed that with increasing concentration of $PbTiO_3$ the presence of the Ti^{4+} ions suppresses the tendency of a 1:1 ordering of the Mg^{2+} and Nb^{5+} cations at the B-site of the perovskite lattice [11]. The dimensions of our coin-shaped samples were 91.6 mm^2 × 0.8 mm and their large surfaces were electroded with gold.

The linear (χ) and the non-linear (χ''_{nl}) susceptibility were measured using an HP 4284A LCR meter in a frequency range from 20 Hz to 1 MHz. We applied ac electrical fields with rms. amplitudes of 6 V/cm and 250 V/cm for the linear and the non-linear measurements, respectively. The latter value turned out to be large enough for the observation of significant non-linear effects in PMN-10PT. We started each measurement with a freshly annealed sample at 380 K which was then cooled with a constant rate to the aging temperature $T_{\rm age}$. Cooling rates were chosen within a range of 0.1 K/min up to approximately 100 K/min. During all dielectric experiments the sample temperature was stabilized by means of a custom-made nitrogen-cooled sample holder ("dipstick"). Since the sample holder could be positioned either in the liquid nitrogen bath or above its surface very slow as well as very fast cooling rates could be handled with high accuracy. For moderate cooling rates the aging temperatures could be stabilized at $T_{\rm age}$ within 300 s with an accuracy better than ±0.01 K. After a temperature quench (cooling rate 100 K/min) it took about 1000 s to stabilize the temperature within ±0.03 K.

3 Experimental results

To characterize the PMN-10PT ceramics the real and the imaginary parts of the linear complex susceptibility (χ' and χ'') were measured during continuously cooling the sample with a cooling rate of 0.5 K/min in the temperature range between 380 K and 220 K. The data showed the typical relaxor properties in agreement with published data [23,30,42]. We will focus on the results obtained for the imaginary part χ'' of the susceptibility, since for the real part χ' the observed effects were qualitatively similar but significantly smaller. All aging experiments presented in the following were carried out around and below the maximum in χ'' as measured in the audio frequency range. The two samples investigated for this study exhibited their maximum value of χ'' at slightly different temperatures (at 280 K and 278 K for a measuring frequency of 20 Hz). This difference is probably caused by small deviations in the PT content of the samples. A shift in the maximum from χ'' of 2 K would correspond to a difference in the PT content of about 0.5% [43].

3.1 Isothermal aging of the linear susceptibility

Figure 1a–c shows the aging behavior of the imaginary part of the linear susceptibility χ'' at the three different aging temperatures 280, 250, and 220 K. The results were obtained after cooling the PMN-10PT sample with a constant cooling rate (0.5 K/min) from 380 K to

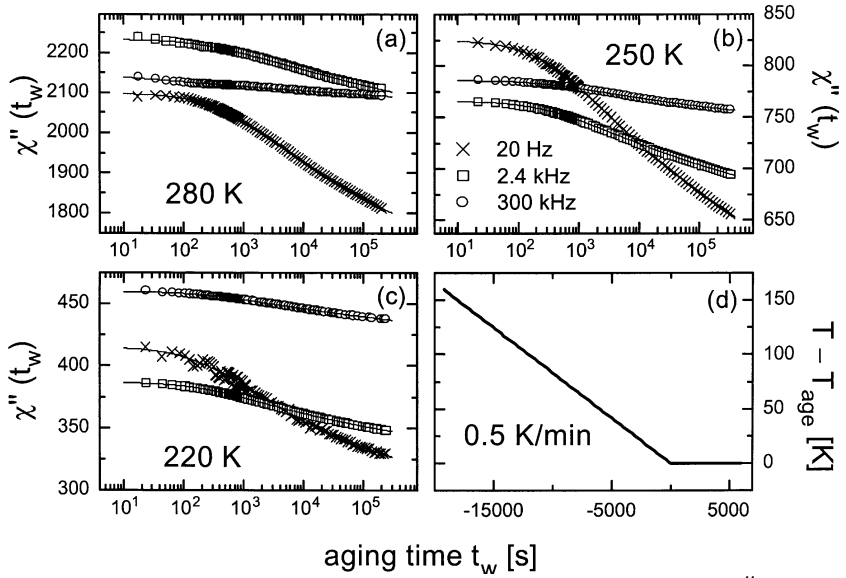

Fig. 1. Isothermal aging as monitored *via* the imaginary part of the dielectric susceptibility χ'' of PMN-10PT for three different frequencies at $T = 280$ K (a), 250 K (b) and 220 K (c). The solid lines in frames (a–c) represent fits using equation (1). The cooling rate prior to aging was chosen to be 0.5 K/min (d).

$T_{\rm age}$ (Fig. 1d). With increasing aging time χ'' steadily decreases for all temperatures and frequencies (20 Hz $< \nu <$ 300 kHz). Even for aging times longer than 2×10^5 s χ'' did not reach its equilibrium value for all $T_{\rm age}$. In the observed time regime all aging curves can be well described by a power law of the form [44,45]

$$\chi''(\omega, t_w) = \chi''_\infty(\omega) + \Delta\chi'' \left[t_0/(t_w + t_0)\right]^a . \qquad (1)$$

Here $\chi''_\infty(\omega)$ denotes the contribution for infinitely long aging time $t_w \to \infty$ and $\Delta\chi''$ is the "strength" of the aging process, *i.e.*, the difference between the instantaneous contribution $\chi''(\omega, t_w = 0)$ and the equilibrium value $\chi''_\infty(\omega)$. A finite time is needed to stabilize the sample at the aging temperature $T_{\rm age}$. Therefore at first glance the parameter t_0 seems to measure the uncertainty in the exact start of the isothermal aging experiment. In order to test this conjecture it is instructive to compare the value of t_0 for all aging temperatures. For the lowest frequency of 20 Hz the parameter t_0 is 445 s at 280 K and continuously reduces to 303 s at 250 K and 205 s at 220 K. However, in our experiments it took always the same time to stabilize the sample temperature at 280, 250, and 220 K. Therefore these findings imply that t_0 has to be regarded as a further parameter for the description of the aging behavior. A similar feature was observed in the aging behavior of the real part of the susceptibility χ' for the orientational glass $K_{1-x}Li_xTaO_3$ [44].

The cooling-rate dependence of the aging in PMN-10PT was investigated for different temperature programs. First, we analyzed how the choice of different cooling rates – which were held constant between 380 K and $T_{\rm age}$ – affect the aging process. To do so we cooled the sample with four different cooling rates ranging from 0.1 K/min to approximately 100 K/min and recorded χ'' at $T_{\rm age}$. The result for an aging temperature of 220 K is shown in Figure 2a for a frequency of 20 Hz. Similar results were obtained also for higher frequencies, but they do not show additional features and therefore they are not shown here.

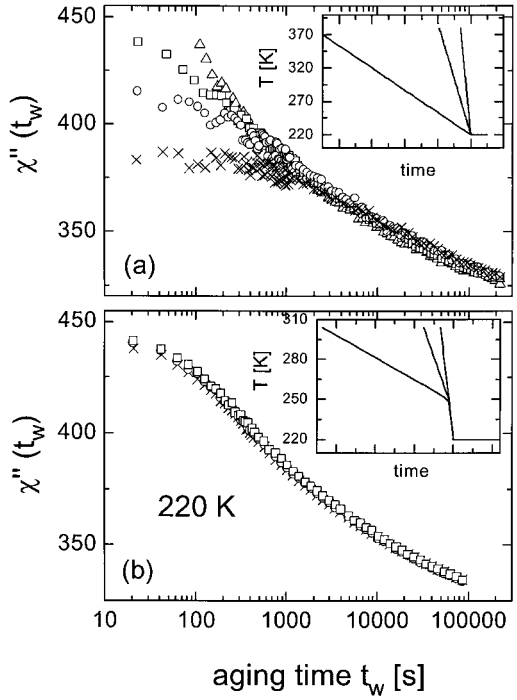

Fig. 2. Isothermal aging revealed by the dielectric susceptibility χ'' of PMN-10PT recorded at a frequency of 20 Hz. Different cooling rates were applied prior to aging: × (0.1 K/min), ○ (0.5 K/min), □ (1.5 K/min), and △ (100 K/min). The insets in frames (a) and (b) show the cooling program. In (a) the rate was chosen to be constant in the whole cooling regime. In frame (b) between 250 K and 220 K the cooling rate was set to 1.5 K/min for all measurements.

It can be recognized clearly that for t_w longer than about 1000 s the susceptibility χ'' does not depend on the

previously applied cooling rate. However, slower cooling yields smaller values of χ'' in the short time regime ($t_w \leq$ 1000 s). A similar dependence on the cooling rate of the susceptibility at the beginning of aging was also observed, *e.g.*, in the magnetic spin glass $CdCr_{1.7}In_{0.3}S_4$ [46,47]. For smaller cooling rates the system seems to be somewhat more aged when reaching $T_{\rm age}$ than it appears for higher rates. In PMN-10PT the parameter t_0 in equation (1) becomes zero for cooling rates $\geq$1.5 K/min. Thus aging proceeds according to the power law $\chi''(\omega, t_w) = \chi''_\infty(\omega) + \Delta\chi'' t_w^{-a}$ for all accessible t_w. These findings conform to the above interpretation of t_0 as a further parameter describing the isothermal aging of χ'' in PMN-10PT. To summarize we observed that for times $t_w \leq t_0$ a dependence on the cooling rate is observable while for longer times the cooling rate does not affect the aging process any more.

In order to find out whether the cooling rate dependence originates from the temperature regime in which the properties change from paraelectric to relaxor ferroelectric we employed another cooling program. Figure 2b shows the aging of the susceptibility χ'' after cooling the sample with different cooling rates in the temperature range between 380 K and 250 K (*i.e.* while passing through the peak in χ'') but keeping the cooling rate constant at 1.5 K/min between 250 K and 220 K. No difference in the aging behavior between the rates of 0.1 K/min, 0.5 K/min and 1.5 K/min can be seen. This implies that the cooling rate affects the aging in PMN-10PT only in the temperature interval close to $T_{\rm age}$. It is irrelevant for the subsequent aging how fast the sample is cooled when passing the peak in χ''.

3.2 Scaling of the linear and of the non-linear susceptibility

In magnetic spin glasses it is typically observed that the time dependent linear susceptibility χ does not depend on the aging time t_w and on the frequency ω separately. Rather χ shows scaling with ωt_w, *i.e.* the aging part of the susceptibility follows one master curve for all ω [40,46]

$$\chi(t_w, \omega) = \chi_\infty + \Delta\chi \frac{c}{(\omega t_w)^a} \cdot \qquad (2)$$

Here c is a dimensionless parameter. An ωt_w-scaling according to equation (2) was also observed in the aging of the linear susceptibility in a PMN single crystal [39,48] while it could not be found in a $K_{1-x}Li_xTaO_3$ crystal [49] for temperatures well below the glass transition. The scaling in spin glasses can only partly be ascribed to the very broad distribution of relaxation times in these materials. Merely it is believed that an ωt_w-scaling is caused by the fact that the processes leading to the observed aging behavior and the underlying mechanisms of the response function are strongly coupled to one another or even of the same origin, see the discussion relating to hierarchical spin glass scenarios [50]. In Figure 3a the linear susceptibility $\chi''(t_w, \omega)$ of PMN-10PT is plotted against the frequency-scaled aging time ωt_w. Neither at a temperature of 250 K nor at 220 K a scaling can be observed. To further test scaling properties of χ'' in PMN-10PT we recorded the t_w-dependent non-linear susceptibility χ''_{nl}. The result for an ac electric field amplitude of 250 V/cm is shown in Figure 3b. In contrast to the linear susceptibility χ''_{nl} shows nearly perfect ωt_w-scaling at a temperature of 220 K.

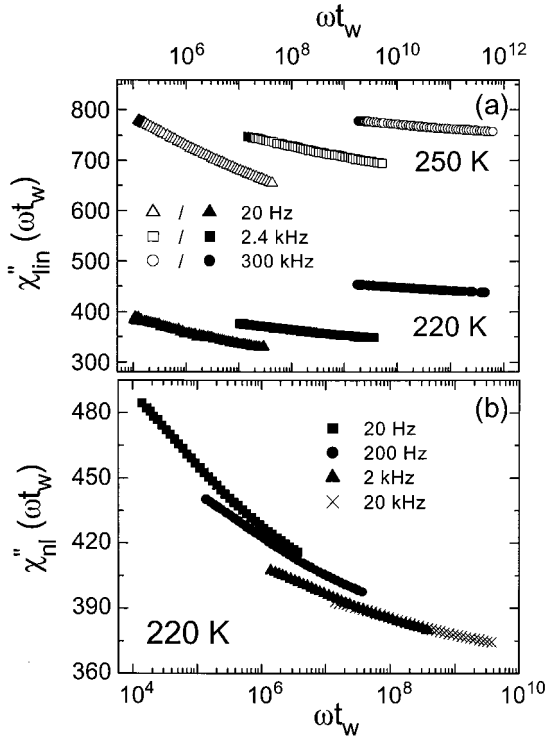

Fig. 3. Isothermal aging as seen in the susceptibility χ''. The data are plotted against the scaled aging time ωt_w. In (a) the linear susceptibility is shown for 250 K and 220 K while in (b) the non-linear susceptibility is plotted.

3.3 Memory effect after aging at a single temperature

We have already presented the isothermal aging behavior of the susceptibility χ'' (see Figs. 1 and 2) at a single temperature $T_{\rm age}$. χ'' steadily decreases with increasing waiting time after cooling the sample to $T_{\rm age}$. This behavior is due to the fact that the system evolves towards equilibrium. In the following we investigate how this incomplete aging process at $T_{\rm age}$ affects χ'' on further cooling and on subsequent re-heating.

In Figure 4 it is shown that upon further cooling (subsequent to aging) one finds that χ'' at first increases and 3–5 K below $T_{\rm age}$ merges again with the reference curve of χ'', a feature commonly called rejuvenation [47]. Here the reference curve, called $\chi''_{\rm ref}$, was measured during continuously cooling the system without aging. So the aging at $T_{\rm age}$ obviously does not affect the behavior of χ'' at temperatures considerably lower than $T_{\rm age}$. After cooling the system to 260 K (curve 1) or to 220 K (curve 2) we immediately re-heated the system at a rate of 0.5 K/min. In the temperature range around $T_{\rm age}$ we observed that χ'' shows

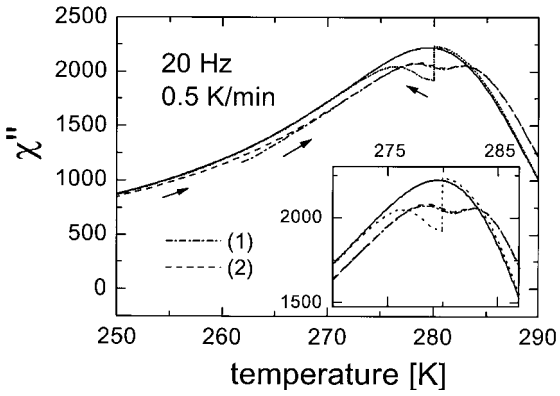

Fig. 4. Rejuvenation and memory effect after aging for 200 000 s at 280 K. On cooling below the aging temperature of 280 K the χ'' curve (dotted line) eventually merges with the reference curve (solid line). On re-heating the curves reveal a memory effect with a maximum in χ'' at 281 K for cooling 60 K (dashed line, curve 2) and for cooling 20 K (dash-dotted line, curve 1) below 280 K. The reference curve $\chi''_{\rm ref}$ was measured on continuously cooling with a rate of 0.5 K/min. The inset gives a magnified view of χ'' near $T_{\rm age}$.

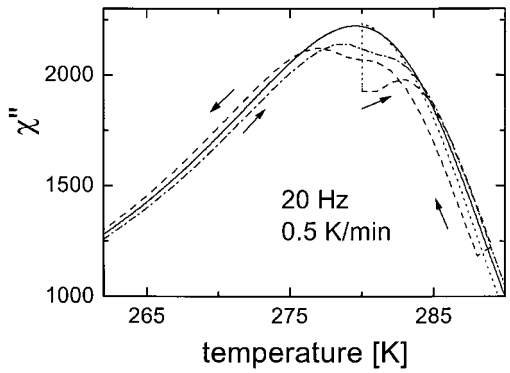

Fig. 5. Rejuvenation and memory effect after aging for 200 000 s at 280 K. In contrast to Figure 4 at the end of the aging period the temperature was increased by 10 K and then the sample was immediately cooled below 280 K (dashed line). A memory to the former aging is seen with a maximum in χ'' around 279 K. On re-heating (dash-dotted line) a memory effect appears, albeit weaker than shown in Figure 4, with a maximum at 281 K. The reference curve $\chi''_{\rm ref}$ is the same as shown in Figure 4 (solid line).

a dip below the reference curve $\chi''_{\rm ref}$. Since $\chi''_{\rm ref}$ was measured during continuously cooling at a rate of 0.5 K/min from 380 K to about 200 K it represents the instantaneous (*i.e.*, $t_w = 0$) contribution to the susceptibility. This means that a *memory* to the configuration adopted during the previous aging process remains even after cooling the system to a temperature 60 K below $T_{\rm age}$. Similar memory effects were also found in spin glasses [51,52], in a PMN single crystal [39], and in a polymer glass below $T_{\rm g}$ [53]. They were not observed in a PMN-30PT ceramic [39].

During the subsequent heating a dip in χ'', *i.e.* the signature of the memory effect, appears about 1 K above the former aging temperature. Looking closer at Figure 4 one can observe that the re-heating curve (2) starts to deviate from the reference curve at ∼250 K provided that the sample is cooled below that temperature after aging at 280 K. If the specimen is cooled only to 260 K (curve 1) we find analogous results.

A further experiment was done in order to find out whether or not memory phenomena can be observed only when cycling the temperature below $T_{\rm age}$ (this will be called a *negative* cycle). A *positive* temperature cycle was carried out for PMN-10PT as follows: after aging at $T_{\rm age}$ = 280 K for 200 000 s we heated the sample to a temperature about 10 K above $T_{\rm age}$ and immediately lowered the temperature to $T_{\rm age} - 25$ K. In both cases the magnitude of the ramping rate was 0.5 K/min. The result is depicted in Figure 5. During the cooling process a memory to the former aging can be seen which is almost as strong as the memory effect observed after cooling the system below the former aging temperature (Fig. 4). When re-heating the system this memory effect is yet again observed, however less pronounced and with its maximum shifted to a slightly higher temperature. Consequently these findings indicate a more or less symmetric memory behavior for undercooling or overheating after aging at 280 K. So far a memory to aging after heating and immediately cooling back to the previous aging temperature has in a similar way only be observed in the relaxor ferroelectric PLZT 9/35/65 [39].

3.4 Aging at two temperatures – temperature cycles

In the following the memory effect discussed above is further explored. After cooling with a constant rate of 0.5 K/min from T = 380 K we first aged the relaxor PMN-10PT at the temperature T_1 (aging time t_1), interrupted the aging at T_1 by a temperature jump to T_2 (a few K below or above T_1), and aged at that temperature (aging time t_2). Finally, the sample was returned to the initial aging temperature T_1 (aging time t_3). During the entire procedure the time dependence of the susceptibility χ'' was recorded. Similar temperature cycle experiments have already been done on spin glasses [54], on the relaxor PMN [39], and on the orientational glasses $K_{1-x}Li_xTaO_3$ [44,55] and $KTa_{1-x}Nb_xO_3$ [56].

Figure 6a shows the result of a negative temperature jump followed by a positive one for T_1 = 280 K and T_2 = 278 K (*negative* temperature cycle). The aging time t_1 was 50 000 s and t_2 was 15 000 s. At T_1 the system slowly evolves to its equilibrium value and χ'' reduces according to a power law (Eq. (1)). Obviously the temperature change to 278 K initializes new aging processes at $t_2 = 0$. The initial value $\chi''(278\ {\rm K}, t_2 = 0)$ is somewhat smaller (approximately 5%) than the reference value $\chi''_{\rm ref}(278\ {\rm K})$ [57] (*cf.* Figs. 6 and 4). The 5% decrease may be taken to imply that the prior aging at 280 K has yielded a configuration which appears somewhat more aged than that corresponding to the reference (effectively $t_w = 0$) measurement $\chi''_{\rm ref}$. The jump back to the temperature T_1 yet again leads to the initialization of new aging processes. But $\chi''(t_3 = 0)$ is significantly smaller

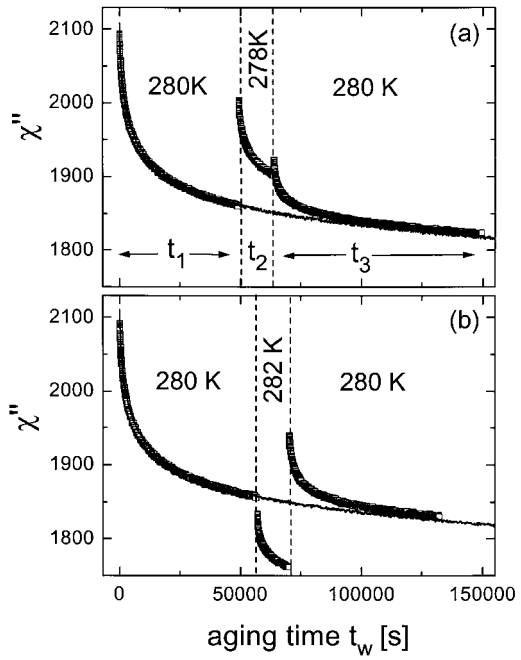

Fig. 6. Aging as evident from the susceptibility χ'' during (a) a negative and (b) a positive temperature cycle at 280 K with $|\Delta T| = 2$ K. The solid lines in (a) and (b) were measured during aging at 280 K without temperature cycling. All data were recorded at a frequency of 20 Hz.

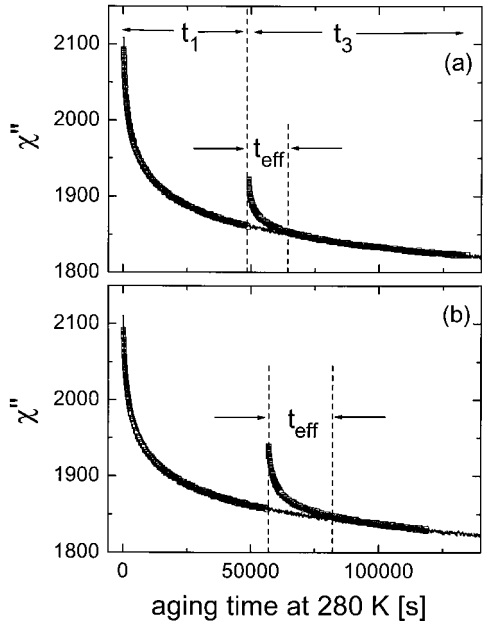

Fig. 7. Aging as seen in the susceptibility χ'' at 280 K exclusively, *i.e.* the data corresponding to the aging times t_2 (*cf.* Fig. 6) are cut out. The effective aging times $t_{\rm eff}$ of (a) the positive and (b) the negative cycle, are marked by arrows.

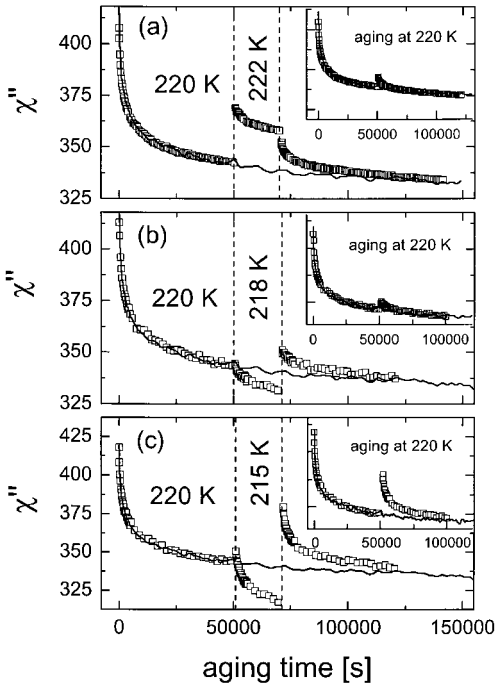

Fig. 8. Same as Figures 6 and 7 except that the base temperature was chosen to be 220 K. ΔT was (a) +2 K, (b) −2 K, and (c) −5 K. All data were recorded at 20 Hz.

than $\chi''(t_1 = 0)$, *i.e.* a part of the system remains in the configuration adopted at the end of the aging time t_1. For comparison the result of a positive temperature cycle 280 K – 282 K – 280 K ($t_1 = 56\,000$ s, $t_2 = 15\,000$ s) is depicted in Figure 6b. After the temperature jump to T_2 the susceptibility χ'' is now even smaller than χ'' at the end of the aging interval at 280 K. This feature is due to the fact that here for the initial values of the susceptibility the relation $\chi''_{\rm ref}(278\,{\rm K}) > \chi''_{\rm ref}(280\,{\rm K}) > \chi''_{\rm ref}(282\,{\rm K})$ holds. The aging measurements of the last chapter (*cf.* Figs. 4 and 5) were made with a different sample that showed the maximum of χ'' at a slightly higher temperature. Otherwise the behavior is similar to that after a negative temperature jump.

Figure 7 shows the composite aging behavior at 280 K exclusively (a) for the negative and (b) for the positive temperature cycle, *i.e.* with the data recorded at temperature T_2 cut out. In addition a reference curve $\chi''(t_w)$ measured after cooling to 280 K without performing additional temperature jumps is plotted. Except for a time $t_{\rm eff}$ (covering the initial regime of t_3) the composite and the reference curves are identical, independent of the size of the (cut-out) temperature jumps. Thus it is seen that at T_2 new aging processes are initialized which, however, decay during the relatively short period $t_{\rm eff}$. This implies that only relatively fast relaxation processes can "react" to the temperature jumps. Processes slower than t_2 (or $t_{\rm eff}$) remain essentially frozen. Except for the difference in the value of the effective aging time $t_{\rm eff}$ ($\cong$16 000 s for a negative and $\cong$25 000 s for a positive temperature cycle) PMN-10PT exhibits a symmetric aging during negative and positive temperature cycles for $T_1 = 280$ K and temperature jumps of 2 K.

Negative and positive temperature cycles were also done at a significantly lower aging temperature of 220 K. Figure 8 shows the results for (a) a negative and (b) a positive cycle with temperature jumps of 2 K. The insets present the aging at 220 K exclusively. Qualitatively

Table 1. The following parameters for negative ($\Delta T < 0$) and for positive ($\Delta T > 0$) temperature cycles are compiled. First the effective aging time $t_{\rm eff}$ originating from measurements performed after two opposing temperature jumps and then the absolute changes of the susceptibilities $\Delta\chi''_{ij} = \chi''(t_j = 0) - \chi''(t_i = \max)$ observed when stepping the temperature (*cf.* Figs. 6, 7, and 8). The last two columns give the initial contributions to $\chi''(T_j, t_j = 0)$ subsequent to the temperature jumps. These data are normalized to the initial contribution at that temperature without temperature cycling, $\chi''_{\rm ref}(T_j, t_w = 0)$.

$T_{\rm age}$ / K	ΔT / K	$t_{\rm eff}$ / s	$\Delta\chi''_{12}$	$\Delta\chi''_{23}$	$\Delta\chi''_{13}$	$\frac{\chi''(T_2,t_2=0)}{\chi''_{\rm ref}(T_2)}$	$\frac{\chi''(T_3,t_3=0)}{\chi''_{\rm ref}(T_3)}$
280	−2	≅16 000	144	14	62	0.95	0.92
280	+2	≅25 000	–22	177	82	0.95	0.93
220	−2	≅15 000	2	20	9	0.88	0.86
220	+2	≅15 000	27	–6	10	0.88	0.86
220	−5	$> t_3$	7	72	37	0.93	0.91

no difference can be seen compared to the behavior at 280 K. For both negative and positive temperature jumps $t_{\rm eff}$ is about 15 000 s. A difference to the behavior at 280 K can only be observed in the initial values $\chi''(t_2 = 0)$ and $\chi''(t_3 = 0)$ at the beginning of the second and of the third aging interval, respectively. After the temperature jump from 220 K to 218 K $\chi''(t_2 = 0)$ shows essentially no change (*i.e.* $\Delta\chi''_{12} = 2$) in contrast to what is observed for a temperature jump from 280 K to 278 K ($\Delta\chi''_{12} = 144$). The relevant absolute changes of χ'' after the temperature jumps are denoted as $\Delta\chi''_{12}$ and $\Delta\chi''_{23}$ [58].

Table 1 summarizes the absolute changes $\Delta\chi''_{12}$, $\Delta\chi''_{23}$, and $\Delta\chi''_{13}$ and the values of the initial contributions to the susceptibility after the temperature jumps normalized to the initial contribution at each temperature without performing temperature jumps [$\chi''_{\rm ref}(T_{\rm i})$]. On the one hand, it can be seen that the sum of the susceptibility changes $\Delta\chi''_{12} + \Delta\chi''_{23}$ approximately coincides for positive and negative temperature cycles for the starting temperatures 280 K and 220 K. On the other hand, positive and negative temperature cycles lead to a slightly different configuration at the beginning of the aging interval t_3 at 280 K (the effective aging times $t_{\rm eff}$ and the changes $\Delta\chi''_{13}$ differ significantly) while at 220 K the symmetry between positive and negative cycles is more perfect (*cf.* the values for $t_{\rm eff}$ and $\Delta\chi''_{13}$).

We want to emphasize that the values of $\Delta\chi''_{12}$ and $\Delta\chi''_{23}$ in PMN-10PT for positive and negative cycles (see Tab. 1) are mainly determined by the initial values $\chi''_{\rm ref}(T_i, t_w = 0)$, in contrast to the behavior, *e.g.*, in $K_{1-x}Li_xTaO_3$ [55]. There $\Delta\chi'$ was nearly constant for temperature jumps of the same magnitude, irrespective of whether they were positive or negative.

Compared to the temperature cycles at 280 K the reinitialization of new aging processes by temperature jumps is less pronounced in the temperature range around 220 K. This results in lower initial values of χ'' subsequent to a temperature jump as compared to the initial value of χ'' of the reference measurement (see the last two columns in Tab. 1).

Finally Figure 8c shows the imaginary part of the susceptibility χ'' during a negative temperature cycle with temperature jumps of 5 K. It can be seen that after the temperature changes the re-initialization of new aging processes is more pronounced than for smaller temperature jumps. A continuation of the aging processes started in the time interval t_1 could not be observed at the end of the temperature cycle as it was observed for smaller temperature jumps.

4 Discussion and concluding remarks

Recently an interpretation of the aging behavior of the real part of the susceptibility χ' in the disordered paraelectric phase of the orientational glass $K_{1-x}Li_xTaO_3$ was given within a specific model [59]. In this model the slow decay of the dielectric susceptibility in $K_{1-x}Li_xTaO_3$ was associated with the growth of domains, leading to a reduced density of domain walls. The motion of the walls strongly slows down with decreasing temperature because they are hindered by static random fields which are frozen on the experimental time scale. The aging behavior within that model is described by the sizes R of the domains alone. These are limited by a temperature dependent correlation length $\xi(T)$ characterizing the domains in equilibrium. In a further investigation dealing with aging in the disordered ferroelectric $KTa_{1-x}Nb_xO_3$ [60] the model was modified by assuming that the configuration of the domain walls as well (and not only of the domain sizes) affect their aging.

Our results from dielectric hole burning experiments on PMN-10PT can also qualitatively be described by a model of movable domain walls the mobility of which is hindered by pinning effects [30]. The dynamics is then governed by a (segment of a) domain wall in an energy landscape of pinning barriers. During aging at a given temperature some domains grow at the expense of others. This reduces the total number of the domains and the overall area of the domain walls. Furthermore wall reconformations on small length scales occur leading to energetically favorable configurations in the free-energy landscape of the pinning barriers. Both contributions cause a steady decrease in the dielectric susceptibility as time evolves. Whether such a domain model is also suitable

to explain the observed features during isothermal aging and during the temperature cycles in PMN-10PT will be discussed in the following.

Let us start by noting that we did not observe a dependence of the aging process on the cooling rate around and below the maximum in χ''. Only the cooling rate in the temperature interval a few kelvin above $T_{\rm age}$ affected the aging of PMN-10PT. Independent of the thermal history all aging curves merge for $t_w > 1000$ s similar to what was found in the spin glass $CdCr_{1.7}In_{0.3}S_4$ [46,47]. The orientational glasses $K_{1-x}Li_xTaO_3$ and $KTa_{1-x}Nb_xO_3$, however, show a significant cooling rate dependence of $\chi(t_w)$ also for long aging times [44,56]. Particularly the manner in which the transition temperature $T_{\rm g}$ is crossed appears to be important for the aging behavior of, *e.g.* $K_{1-x}Li_xTaO_3$. This behavior was considered characteristic of a domain type scenario [59]. The above described finding for PMN-10PT can be interpreted such that domain wall re-conformations play a stronger role than domain growth. Because domains are growing with time a pure domain growth scenario (as observed, *e.g.*, in ferroelectrics) would result in a stronger cooling rate dependence than observed for PMN-10PT [46,51]. Thus the data taken after slower cooling appear to be somewhat more aged (*i.e.*, $\Delta\chi''(t_w)$ is smaller) only at the beginning of aging (Fig. 2).

For PMN-10PT we observed that the scaling of the linear susceptibility differs from that of the non-linear susceptibility (Fig. 3). A complex scaling of $\chi''(t_w)$ arises if the mechanisms leading to the linear dielectric response are different from those responsible for the aging properties. But why does the non-linear susceptibility exhibit scaling? These findings can be rationalized within the domain model. While in the linear regime only local degrees of freedom within distinct domains contribute to the dielectric response, non-linear contributions to the response include the motion of domain walls. As a consequence a scaling of the aging-time dependent non-linear susceptibility χ''_{nl} should be observed indicating that the contribution to the non-linear dielectric response and the processes leading to aging phenomena (growing of domains and reconformation of domain wall segments) are of the same origin.

In the dielectric hole burning investigations [30,31] on the PMN-10PT relaxor we observed an Ωt_w-scaling (with respect to the pump frequency Ω) for the recovery of the dielectric holes. Here t_w denotes the waiting time after the pump process (carried out for temperatures around the peak in χ''). The observed pump-field dependence of the re-equilibration time scale in the hole burning experiments on PMN-10PT confirms the interpretation within a domain-wall scenario. The higher the exciting pump fields are, the stronger is the change of the domain configuration and thus the longer it takes for the domain-wall configuration to re-equilibrate [30].

The behavior of the susceptibility χ'' subsequent to aging at a single temperature (Figs. 4 and 5) and during the temperature cycles (Figs. 6, 7, and 8) revealed that upon re-heating (or re-cooling) some memory of the previous aging at the higher (lower) temperature exists. The most remarkable feature in PMN-10PT is the fact that memory to the former aging configuration can be retrieved even after heating the system 10 K above the aging temperature. To our knowledge a comparable feature has only been observed in the relaxor ferroelectric PLZT, so far [39]. For spin glasses and for orientational glasses memory effects were only reported for negative temperature cycles [54–56]. In these materials positive temperature cycles serve to anneal the sample, *i.e.* aging is restarted after heating the system and cooling it back to the previous aging temperature. The observation of an asymmetric behavior under positive and negative temperature cycles was put forward as a strong argument in favor of the existence of a hierarchical organization of the configurations of the (domain) states in phase space. With decreasing temperature domain walls become fixed on a large spatial scale while re-conformations of small wall segments can still occur in order to minimize the free energy of the pinning configuration [46].

The symmetric behavior observed in PMN-10PT for negative and for positive temperature cycles suggests a more complex scenario. Alternatively, the memory effect showing up for a positive temperature cycle could arise if the time scales associated with the re-conformation of the domain walls (or segments thereof) exhibit a very broad distribution. On cooling (heating) subsequent to the aging process at $T_{\rm age}$ the susceptibility merges with the reference curve suggesting that the effect of the former aging is erased and new aging processes are started. The appearance of a memory on heating (cooling) the system back to $T_{\rm age}$ is plausible if one assumes that the configuration of larger (*i.e.* slower) domain wall segments are frozen on the experimental time scale due to the prior aging process at $T_{\rm age}$. When coming back to $T_{\rm age}$ aging processes are only partly re-initialized. Re-conformation of smaller (*i.e.* faster) domain wall segments then causes the observed rejuvenation in PMN-10PT.

On the basis of measurements of the third-order nonlinear susceptibility it has been argued that a domain scenario (similar to that favored in the present article) should apply to pure PMN only above a critical field of 1700 V/cm [61]. This is about 7 times larger than the maximum fields applied in the present work. For lower fields compatibility with several – but not all – aspects of a spherical random-bond random-field (SRBRF) model describing glassy dynamics was found for several relaxors [61,62].

To summarize, in this paper we presented different aging experiments on the relaxor ferroelectric PMN-10PT. We observed that the isothermal aging of the linear susceptibility does not scale with the measuring frequency. However, the non-linear susceptibility shows nearly perfect ωt_w-scaling. Together with the results of dielectric hole burning [30] this suggests that PMN-10PT behaves like a disordered ferroelectric: The dipolar dynamics is governed by movable domain walls which are pinned by the random-field environment in PMN-10PT. The nearly symmetric appearance of memory to a former aging configuration after negative or after positive temperature

cycles indicates an extremely broad distribution of time scales for the re-conformation of domain wall segments.

We thank the Deutsche Forschungsgemeinschaft (Grant No. Bo1301/4) for financial support and S.E. Park from the Material Research Laboratory of the Pennsylvania State University for supplying the PMN-10PT samples.

References

1. G.A. Smolensky, A.I. Agronovskaya, Sov. Phys. Tech. Phys. **3**, 1380 (1958).
2. T.R. Shrout, J.P. Dougherty, Ceram. Trans. **8**, 3 (1990) and references cited therein.
3. K. Uchino, S. Nomura, L.E. Cross, R.E. Newnham, S.J. Jang, J. Mater. Sci. **16**, 569 (1981).
4. G.A. Smolensky, J. Phys. Soc. Jpn, Suppl. **28**, 26 (1970).
5. L.E. Cross, Ferroelectrics **76**, 241 (1987).
6. E.V. Colla, E.Y. Korreleva, N.M. Okuneva, S.B. Vakhrushev, J. Phys. Cond. Matt. **4**, 3671 (1992).
7. A. Levstik, Z. Kutnjak, C. Filipic, R. Pirc, Phys. Rev. B **57**, 11204 (1998).
8. A.E. Glazounov, A.K. Tagantsev, J. Phys. Cond. Matt. **10**, 8863 (1998).
9. Z. Kutnjak, V. Bobnar, C. Filipic, A. Levstik, Europhys. Lett. **53**, 673 (2001).
10. J. Chen, H.M. Chan, M.P. Harmer, J. Am. Ceram. Soc. **72**, 593 (1989).
11. A.D. Hilton, D.J. Barber, C.A. Randall, T.R. Shrout, J. Mater. Sci. **25**, 3461 (1990).
12. L.A. Bursill, H. Qian, J. Peng, X.D. Fan, Physica B **216**, 1 (1995).
13. I.G. Siny, S.G. Lushnikov, R.S. Katiyar, E.A. Rogacheva, Phys. Rev. B **56**, 7962 (1997).
14. M.E. Marssi, R. Farhi, Y.I. Yuzuk, J. Phys. Cond. Matt. **10**, 9161 (1998).
15. F.M. Jiang, S. Kojima, Phys. Rev. B **62**, 8572 (2000).
16. H. You, Q.M. Zhang, Phys. Rev. Lett. **79**, 3950 (1997).
17. S.B. Vakhrushev, J.-M. Kiat, B. Dkhil, Solid State Commun. **103**, 477 (1997).
18. A. Naberezhnov, S. Vakhrushev, B. Dorner, D. Strauch, H. Moudden, Eur. Phys. J. B **11**, 13 (1999).
19. P. Bonneau, P. Garnier, G. Calvarin, E. Husson, J.R. Gavarri, A.W. Hewat, A. Morell, J. Solid State Chem. **91**, 350 (1991).
20. L.E. Cross, Ferroelectrics **151**, 305 (1994).
21. D. Viehland, S.J. Jang, L.E. Cross, M. Wuttig, Phys. Rev. B **46**, 8003 (1992).
22. S.N. Dorogovtsev, N.K. Yushin, Ferroelectrics **112**, 27 (1990).
23. D. Viehland, S.J. Jang, L.E. Cross, M. Wuttig, J. Appl. Phys. **68**, 2916 (1990).
24. V. Westphal, W. Kleemann, M.D. Glinchuk, Phys. Rev. Lett. **68**, 847 (1992).
25. B.E. Vugmeister, H. Rabitz, Phys. Rev. B **57**, 7581 (1998).
26. R. Blinc, J. Dolinsek, A. Gregorovic, B. Zalar, C. Filipic, Z. Kutnjak, A. Levstik, R. Pirc, Phys. Rev. Lett. **83**, 424 (1999).
27. U.T. Höchli, K. Knorr, A. Loidl, Adv. Phys. **39**, 405 (1990).
28. K. Binder, A.P. Young, Rev. Mod. Phys. **58**, 801 (1986).
29. T. Natterman, Y. Shapir, I. Vilfan, Phys. Rev. B **42**, 8577 (1990) and references cited therein.
30. O. Kircher, G. Diezemann, R. Böhmer, Phys. Rev. B **64**, 054103 (2001).
31. O. Kircher, B. Schiener, R. Böhmer, Phys. Rev. Lett. **81**, 4520 (1998).
32. B. Schiener, R. Böhmer, A. Loidl, R.V. Chamberlin, Science **274**, 752 (1996).
33. R. Böhmer, G. Diezemann, in: *Broadband dielectric spectroscopy*, edited by F. Kremer, A. Schönhals (Springer, Berlin, 2002) in press.
34. R.V. Chamberlin, Phys. Rev. Lett. **83**, 5134 (1999).
35. W. Kleemann, V. Bobnar, J. Dec, P. Lehnen, R. Pankrath, S.A. Prosandeev, Ferroelectrics **261**, 43 (2001).
36. T. El Goresy, O. Kircher, R. Böhmer, Solid State Commun. **121**, 485 (2002).
37. L.C.E. Struik, *Physical Aging in Amorphous Polymers and other Materials* (Elsevier, Amsterdam, 1978).
38. Z. Kutnjak, C. Filipic, V. Bobnar, A. Levstik, Ferroelectrics **240**, 273 (2000).
39. E. Colla, L.K. Chao, M.B. Weissman, Phys. Rev. B **63**, 134107 (2001).
40. J. Hammann, E. Vincent, V. Dupuis, M.O.M. Alba, J.-P. Bouchaud, J. Phys. Soc. Jpn, Suppl. A **69**, 206 (2000).
41. E.V. Colla, N.K. Yushin, D. Viehland, J. Appl. Phys. **83**, 3298 (1998).
42. Z.-Y. Cheng, R.S. Katiyar, X. Yao, A. Guo, Phys. Rev. B **55**, 8165 (1997).
43. S.W. Choi, T.R. Shrout, S.J. Jang, A.S. Bhalla, Ferroelectrics **100**, 28 (1989).
44. F. Alberici, P. Doussineau, A. Levelut, J. Phys. I France **7**, 329 (1997).
45. A fit with a stretched exponential function $\chi''(\omega, t_w) = \chi''_\infty(\omega) + \Delta\chi'' \exp[-(t_w/\tau)^\beta]$ was also possible and yielded exponents $\beta = 0.31 \pm 0.02$. However, the quality of those fits was inferior to those based on equation (1), when considering the entire range of times.
46. J.-P. Bouchaud, in: *Soft and Fragile Matter: Nonequilibrium Dynamics, Metastability and Flow*, edited by M.E. Cates, M.R. Evans (IOP Publishing, Bristol and Philadelphia, 2000), pp. 285–304 and references cited therein.
47. K. Jonason, E. Vincent, J. Hamman, J.-P. Bouchaud, P. Nordblad, Phys. Rev. Lett. **81**, 3243 (1998).
48. E.V. Colla, L.K. Chao, M.B. Weissman, D. Viehland, Phys. Rev. Lett. **85**, 3033 (2000).
49. F. Alberici-Kious, J.-P. Bouchaud, L.F. Cugliandolo, P. Doussineau, A. Levelut, Phys. Rev. Lett. **81**, 4987 (1998).
50. A.T. Ogielsky, D.L. Stein, Phys. Rev. Lett. **55**, 1634 (1985); E. Vincent, J.-P. Bouchaud, J. Hamman, F. Lefloch, Philos. Mag. B **71**, 489 (1995); J.-P. Bouchaud, D.S. Dean, J. Phys. I **5**, 265 (1995).
51. E. Vincent, V. Dupuis, M. Alba, J. Hamman, J.-P. Bouchaud, Europhys. Lett. **50**, 674 (2000).
52. V. Dupuis, E. Vincent, J.-P. Bouchaud, J. Hamman, A. Ito, H. Aruga Katori, Phys. Rev. B **64**, 174204 (2001).
53. L. Bellon, S. Ciliberto, C. Laroche, Europhys. Lett. **51**, 551 (2000).

54. F. Lefloch, J. Hammann, M. Ocio, E. Vincent, Europhys. Lett. **18**, 647 (1992).
55. F. Alberici, P. Doussineau, A. Levelut, Europhys. Lett. **39**, 329 (1997).
56. P. Doussineau, T. de Lacerda-Arôso, A. Levelut, Eur. Phys. J. B **16**, 455 (2000).
57. It should be kept in mind that $\chi''_{\rm ref}$ always refers to $t_w = 0$, *i.e.* the time when the first aging temperature is reached subsequent to cooling from a temperature significantly higher than the peak in χ''.
58. The susceptibility changes are defined as $\Delta\chi''_{ij} = \Delta\chi''(T_i \to T_j) = \chi''(t_j = 0) - \chi''(t_i = \max)$.
59. F. Alberici-Kious, J.-P. Bouchaud, L.F. Cugliandolo, P. Doussineau, A. Levelut, Phys. Rev. B **62**, 14766 (2000).
60. P. Doussineau, T. de Lacerda-Arôso, A. Levelut, J. Phys. Cond. Matt. **13**, 8799 (2001).
61. V. Bobnar, Z. Kutnjak, R. Pirc, R. Blinc, A. Levstik, Phys. Rev. Lett. **84**, 5892 (2000).
62. J.-H. Ko, F. Jiang, S. Kojima, T.A. Shaplygina, S.G. Lushnikov, J. Phys. Cond. Matt. **13**, 5449 (2001).